Available online at www.sciencedirect.com

ScienceDirect

Journal of Nutritional Biochemistry 117 (2023) 109319

Journal of Nutritional Biochemistry

RESEARCH PAPER

Transcriptomics of natural and synthetic vitamin D in human hepatocyte lipotoxicity

Desirée Bartolini[a,b], Linda Zatini[a], Anna Migni[a], Tiziana Frammartino[c], Angela Guerrini[c], Stefano Garetto[c], Jacopo Lucci[c], Isabelle Franco Moscardini[c], Giada Marcantonini[a], Anna Maria Stabile[b], Mario Rende[b], Francesco Galli[a,*]

[a] Department of Pharmaceutical Sciences, University of Perugia, Perugia, Umbria, Italy
[b] Department of Medicine and Surgery, Section of Human, Clinical and Forensic Anatomy, University of Perugia, Perugia, Umbria, Italy
[c] Bios-Therapy, Physiological Systems For Health S.p.A., Loc. Aboca 20, Sansepolcro, Arezzo, Italy

Received 29 July 2022; received in revised form 29 January 2023; accepted 14 March 2023

Abstract

Vitamin D (VD) has been used to prevent nonalcoholic fatty liver disease (NAFLD), a condition of lipotoxicity associated with a defective metabolism and function of this vitamin. Different forms of VD are available and can be used for this scope, but their effects on liver cell lipotoxicity remain unexplored. In this study we compared a natural formulation rich in VD2 (Shiitake Mushroom extract or SM-VD2) with a synthetic formulation containing pure VD3 (SV-VD3) and the bioactive metabolite 1,25$(OH)_2$-D3. These were investigated in chemoprevention mode in human HepaRG liver cells supplemented with oleic and palmitic acid to induce lipotoxicity. All the different forms of VD showed similar efficacy in reducing the levels of lipotoxicity and the changes that lipotoxicity induced on the cellular transcriptome. However, the three forms of VD generated different gene fingerprints suggesting diverse, even if functionally convergent, cytoprotective mechanisms. Main differences were (1) the number of differentially expressed genes (SV-VD3 > 1,25$[OH]_2$-D3 > SM-VD2), (2) their identity that demonstrated significant gene homology between SM-VD2 and 1,25$(OH)_2$-D3, and (3) the number and type of biological functions identified by ingenuity pathway analysis as relevant to liver metabolism and cytoprotection annotations. Immunoblot confirmed a different response of VDR and other VDR-related proteins to natural and synthetic VD formulations, including FXR, PXR, PPARγ/PGC-1α, and CYP3A4 and CYP24A1. In conclusion, different responses of the cellular transcriptome drive the cytoprotective effect of natural and synthetic formulations of VD in the free fatty acid-induced lipotoxicity of human hepatocytes.

Keywords: Vitamin D; Lipotoxicity; Hepatocytes; NAFLD; Transcriptomics; Gene microarray; Nutrigenomics.

1. Introduction

Vitamin D (VD) is the term used to define a group of fat-soluble secosteroids and an essential micronutrient and endogenous product of cholesterol metabolism with important role in the intestinal transport of calcium and in the control of calcium and phosphate levels [1] (Supplementary Fig. S1). Two main forms are found in food, namely VD2 (ergocalciferol) and VD3 (cholecalciferol); VD2 is mainly of plant origin and is usually used as food ingredient or to prepare natural products rich in VD [2], whereas VD3 is found in animal-based food items, such as fish oils, beef, liver, and eggs [1]. Also, VD3 can be synthetized in skin by sunlight exposure, representing approx. 80 % of the endogenous VD. The two forms have the same metabolism and act as prohormones generating bioactive metabolites (Supplementary Fig. S1), namely 25(OH)-D and 1,25$(OH)_2$-D, or calcitriol; among the different VD analogs and metabolites, 1,25$(OH)_2$-D is the most potent VD receptor (VDR) agonist active in the regulation of bone metabolism and PTH secretion [3]. In addition to calcium/phosphate metabolism and bone homeostasis regulation, VD has other, or "extra-skeletal," functions including immunomodulation and anti-inflammatory effects, cell metabolism regulation and cytoprotective effects that have been demonstrated in the vascular epithelium, neuronal cells, and many other cell types and tissues. This pleiotropic activity of VD is the consequence of the ubiquitous expression of VDR and VD metabolic enzymes in human tissues [4,5].

Abbreviations: VD, Vitamin D; FFA, free fatty acids; SM-VD2, Shitake mushroom extract rich in vitamin D2; SV-VD3, Synthetic VD as colecalciferol; NAFLD, non alcoholic fatty liver disease.

* Corresponding author at: Department of Pharmaceutical Sciences, University of Perugia, Pole of Via del Giochetto, Building B, 06126 Perugia, Italy.
E-mail address: francesco.galli@unipg.it (F. Galli).

https://doi.org/10.1016/j.jnutbio.2023.109319

According to international endocrinology guidelines and experts panel opinions that recently defined the strategy to assess the VD status and its reference values [6–8], suboptimal levels of this vitamin (*i.e.*, levels of 25(OH)-D below the bone health safety threshold of 50 nM) are very frequent, even in apparently healthy subjects, and more than one billion of people worldwide present deficient levels (those associated with increase the risk of skeletal symptoms, *i.e.*, 25(OH)-D < 30 nM or 12 ng/mL) [9]. Also, VD deficiency is a common feature of chronic (extra-skeletal) diseases, possibly by the effect of disease mechanisms, comorbidity and drug therapies [10]. These include chronic liver disease, being the liver tissue the site for the hydroxylation of the provitamin generated in the skin by sunlight exposure to form 25(OH)D, a stable circulating form of VD and the precursor of the active metabolite 1,25$(OH)_2$-D that is formed by a second hydroxylation in the kidney. Given that VD undergoes this important biotransformation in the liver, an abnormal VD metabolism and reduced levels of 25(OH)-D are expected in chronic liver disease [11].

On the other hand, low levels of 25(OH)-D have been associated with an increased risk of chronic liver disease, including nonalcoholic fatty liver disease (NAFLD) and nonalcoholic steatohepatitis (NASH) [11], that are becoming the leading cause of liver transplantation in rich and developing regions [12]. NAFLD derives from processes of lipotoxicity and oxidative stress of the liver cells, and it is considered the hepatic manifestation of metabolic syndrome (MS), leading to insulin resistance and alterations of hepatometabolic indicators as liver enzymes, fasting glucose, triglycerides, and cholesterol levels [13,14]. In this respect, VD deficiency appears to sustain insulin resistance and hepatic inflammation, thus representing a risk factor for MS [15,16]. At the same time, VD is demonstrated to contribute important antiproliferative, anti-inflammatory and antifibrotic effects in the liver tissue, thus holding potential both in the prevention and therapy of NAFLD, also preventing its progression to NASH and eventually to cirrhosis and hepatocarcinoma [11,15].

Despite such potential, little is known about the effects of VD on a fundamental pathogenic process of NAFLD, namely liver lipotoxicity. This is a reversible process consisting in the hepatocellular accumulation of exogenous (dietary) and/or endogenous fats, with consequent induction of a pro-oxidant and cytopathic effects [14,17]. Lipotoxicity presents as the excess of sequestration of neutral lipids into lipid droplets. These are highly regulated subcellular compartments that respond to the transcriptional control of specific groups of genes including the PPAR family of nuclear receptors and inducible and constitutive isoforms of perlipin, as PLIN2 [18].

Even greater is the lack of information on the efficacy and mechanism of action of the different forms or formulations of VD that could be used to treat lipotoxicity. Therefore, more preclinical investigation is needed to fill this gap of knowledge starting from studying these aspects in in vitro models of hepatocellular lipotoxicity.

On these bases, we compared the cytoprotective activity of different forms of VD in human liver cells exposed to free fatty acids (FFA)-induced steatosis, a well-established *in vitro* model of lipotoxicity that recapitulates the earliest steps in the cell pathobiology of NAFLD [19,20]. The forms of VD compared in this study were a nutraceutical formulation rich in VD2 (Shitake mushroom extract; SM-VD2), a synthetic formulation containing pure VD3 (SV-VD3), and the bioactive metabolite 1,25$(OH)_2$-D3 that was used as reference molecule. A gene microarray platform and immunoblot were used to explore the effects of these VD formulations on molecular and biological pathways relevant to VD metabolism and lipotoxicity prevention.

2. Materials and methods

2.1. Chemicals

LC/MS grade absolute methanol was from Biosolve (Dieuze, France). Ultrahigh purified water was prepared using a Avidity Ultra water purification system (Mason Technology, Ireland). Formic acid 98–100% for LC-MS LiChropur, sodium hydroxide solution 50% w/w, ethanol absolute, sodium chloride, sodium sulfate, petroleum ether, and diethyl ether were from Sigma-Aldrich (St. Louis, MO) and were analytical grade. The high-purity external standards used for the preparation of calibration curves were from Sigma-Aldrich (St. Louis, MO, USA) or LGC Standards S.r.l. (Milan, Italy). The Vitamin D3-d3 internal standard was from Sigma-Aldrich (St. Louis, MO, USA). The internal lock masses [purine and HP-0921, hexakis 1H,1H,3H-tetrafluoropropoxy] phosphazine) and tune mix for calibrating the qToF-MS (ESI-low concentration tuning mix) were from Agilent Technologies (Santa Clara, CA, USA). Reagents for cell culture experiments and cell biology and biochemistry assays are described later in the specific subsections.

2.2. Shitake mushroom extract preparation

A freeze-dried extract of Shitake mushroom (cod ABO-AR-2017-691) was prepared in a round bottom flask combining 0.5 g of crude sample with 30 mL of ethanol and 5 mL of an aqueous solution containing 50% of NaOH. After overnight stirring, the sample was transferred to a 150 mL falcon and then centrifuged at 4.000 rpm for 5 minutes. The supernatant was transferred to a separating funnel and extracted with two aliquots (60 mL each one) of diethyl ether: petroleum ether 1:1. The organic layer was purified by washing with two aliquots (50 mL each) of water containing 0.26 mg/mL NaCl. The sample was then freeze-dried trough sodium sulfate using a rotavapor system. The final dried sample was solubilized in 5 mL of methanol and filtered with a 0.22 μm syringe filter (Millipore) before analysis of VD2 levels (Section 2.3) that in the batches of Shitake extract prepared for this study corresponded to 1352 mg/kg.

2.3. LC-QTOF analysis of vitamin D

Ergocalciferol (VD2) levels were assessed in Shitake mushroom extract by using a 1,290 Infinity ultrahigh performance liquid chromatography (UHPLC) system coupled to a 6,545-quadrupole time-of-flight (qToF) high resolution (2 GHz) mass spectrometer equipped with a Dual AJS ESI electrospray ionization source (Agilent Technologies, Santa Clara, CA, USA). The analytical column was a Cortecs C18 column (100 × 2.1 mm, 1.6 μm particle size) protected by a Cortecs C18 VanGuard precolumn (5 × 2.1 mm, 1.6 μm) both supplied by Waters (Milford, MA, USA). The column oven was maintained at 15°C. The chromatographic analysis was performed at flow rate of 0.3 mL/min using H2O + 0.1% HCO_2H (v/v) as mobile phase A and CH_3OH + 0.1% HCO_2H (v/v) as mobile phase B and the following elution gradient: 0.0–6.0 min A/B 5:95; 6.0–12.0 min A/B 4:96; 12.0–16.0 min A/B 4:96. Post run conditioning was performed with A/B 7:93 with a post-time set at 2.0 min. Needle wash parameters: wash needle with methanol for 5 s, wash needle with water for 5 s, wash needle with two-propanol: water 50:50 for 5 s. The injected volume was 5 μL. Mass spectrometry was performed in positive ionization and AIF mode with a scan range from 50–1700 m/z. The system was calibrated and tuned according to the protocols recommended by the manufacturer. Nitrogen (purity > 99.999%) was used as a sheath gas and drying gas at a flow of 12 and 11 L/min, respectively. The sheath and drying gas temperatures were set at 350°C and 325°C, respectively, with the nebulizer pressure at 35 psig and capillary voltage at 3500 V. Fragmentor voltage was 100 V, Skimmer voltage was 65 V and Oct RF Vpp was 750 V. An internal lock mass mixture (Agilent Technologies) was prepared at a final concentration of 4.5 μM purine ($C_5H_4N_4$) and 0.125 μM HP-0921 ($C_{18}H_{18}O_6N_3P_3F_{24}$) by appropriate dilution in methanol/water (95:5, v/v). MassHunter software version B.09 (Agilent Technologies, Santa Clara, CA, USA) was used for data acquisition and processing. The internal lock mass mixture was constantly infused at a flow rate of 0.05 mL/min using an isocratic pump together with the LC eluent for constant mass correction (positive ionization mode: purine [m/z 121.0509], HP-0921 [m/z 922.0098]) to obtain accurate mass time-of-flight data (mass accuracy <5 ppm). A data processing method for targeted screening was produced with the Agilent qToF "Quantitative analysis" software using precursor and product ion information, and the identification of Ergocalciferol present in samples was performed by comparison of MS/MS spectra of the pure reference standard. Compound identification was scored using the high-resolution mass, isotope abundance, the isotope spacing and retention time. Product ions (from 20, 30, and/or 40 eV) were chosen as qualifier in the following order of priority: (1) the most abundant and (2) the most characteristic. A quantifier ion (precursor ion), qualifier ion(s) (product ions), and RTs were merged in the data processing method accepting a retention time shift of 0.3 min.

For sample analysis, calibration curves were prepared by diluting the Shitake extract prepared as described earlier with methanol (from 1:2–1:1000 vol/vol) to obtain aliquots with a final volume of 200 μL. Ten micriliter of internal standard (concentration 0.004 mg/mL) were added to each dilution aliquot. Quantitative data were obtained using a regression curve of pure Ergocalciferol (external standard

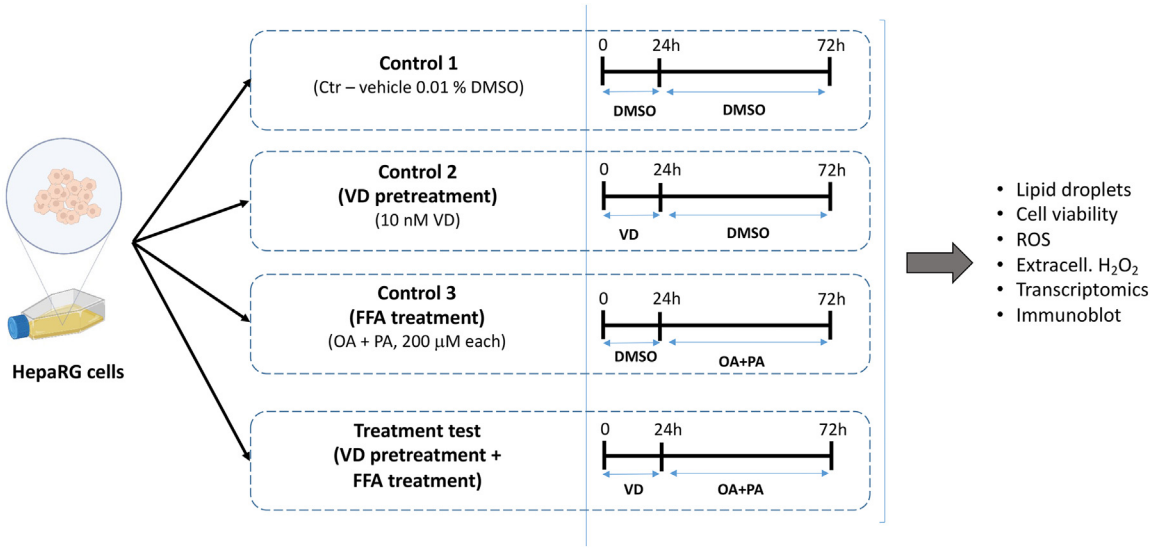

Fig. 1. Study protocol. The chart shows the experimental design of this *in vitro* study performed in HepaRG human liver cells. This included three control tests and one treatment test that were set to assess separate or combined the effect of the 24-h pretreatment step with VD formulations and of the 48-h treatment with FFA to induce lipotoxicity. Further details are reported in the text.

method) monitoring the precursor ion m/z 397.3465. The acquisition of the calibration curves and the acquisition of the sample under investigation were performed in AIF mode acquiring a single high-resolution full scan in three sequential experiments at CE 20, 30, and 40 eV. The data acquisition rate was 2 scans/s and the time was 500 ms/spectrum.

2.4. Cell line and treatments

HepaRG, human progenitor hepatic cells (Thermo Fisher Scientific) were maintained in culture following manufacturer's recommendations. The cells were grown in William's E medium (Thermo Fisher Scientific) supplemented with Glutamax (Gibco), 5 μg/mL human insulin (Lonza) and 50 μM hydrocortisone hemisuccinate (Sigma-Aldrich). Cells were seeded at a density of 10,000 cells/well and kept at 37°C in a humidified 5% CO_2 incubator and were used between passage two and ten (passages were implemented by trypsin-EDTA, Euroclone). Cell treatments were as described in Fig. 1 and included a 24-h pretreatment phase with the VD formulations and a 48-h treatment phase with FFA to induce steatosis and lipotoxicity (described later in more detail); considering control treatments with the vehicle DMSO, the following test combinations are obtained:

1. Control test one– this is to assess the effect of the vehicle DMSO; the cells were pretreated and then treated with the vehicle.
2. Control test two – this test verifies the effect of VD formulations only; the cells were pretreated with the different VD formulations and then treated with the vehicle DMSO.
3. Control test three – this is to verify the effect of lipotoxicity; the cells were pretreated with the vehicle DMSO and then treated with FFA.
4. treatment test – this is the experimental test designed to assess the cytoprotective effect of the VD formulations on the lipotoxicity effect of FFA (assessed in the control test three); the cells were pretreated with the VD formulations and then treated with FFA.

Therefore, to assess biochemistry and microarray data, the different datasets were first normalized for control test one, and the resulting data were used to assess statistical differences between the datasets of treatment test four and control test three.

2.4.1. Pretreatments with vitamin D formulations

HepaRG cells at 70% confluence were incubated for 24 h with either the vehicle (DMSO, Sigma-Aldrich; final concentration in the cell culture medium of 0.001% vol/vol) or VD that was used under three different forms:

1. Shitake mushroom extract rich in vitamin D2 (SM-VD2) prepared and evaluated as described in the Sections 2.2 and 2.3.
2. Synthetic VD as colecalciferol (SV-VD3) (ABIOGEN PHARMA S.p.A, Pisa).
3. 1,25-$(OH)_2$-D3 (Cayman Chemical, CAS No.32222-06-3).

Pretreatments with VD formulations were preliminarily investigated for their intrinsic cytotoxicity and induction of steatosis (not shown), and a final concentration of 10 nM VD in the cell culture medium (as VD2 or VD3 in the case of SM-DV2 and SV-VD3 formulation, respectively) was selected to avoid these drawbacks.

2.4.2. Treatment with FFA

After pretreatment with VD formulations, steatosis was induced by the incubation of HepaRG cells for 48 h with a cocktail of oleic acid (OA; Sigma-Aldrich, product number: O1383) and palmitic acid (PA, Sigma-Aldrich, product number P0500) both used at the final concentration of 200 µM in the culture medium. Stock solutions (200 mM) of OA and PA were prepared in ethanol and isopropanol, respectively, and were diluted in William E complete medium containing 10% FBS to prepare the working solutions. The latter were gently shaken at 40°C for 20 min before being filtered through a 20-μm membrane for the supplementation in the culture media.

2.5. Cell viability

Cell viability was assessed by MTT test (Sigma-Aldrich) according to [21] in 96-well plates. Briefly, after pretreatment with VD formulations and treatment with OA and PA, the cells were incubated for 3 h at 37°C with fresh medium containing the MTT solution. Then, the formazan crystals were dissolved in MTT solubilization solution (10% Triton X-100 plus 0.1 N HCl in anhydrous isopropanol) and the absorbance was recorded at 570 nm in a microplate reader (DTX880, Multimode Detector Beckman Coulter). Other details and calculation of cell viability data were made according to [22].

2.6. Cellular reactive oxygen species

Cellular levels of reactive oxygen species (ROS) were measured by the oxidative conversion of the intracellular probe 2′,7′-dichlorofluorescein-diacetate (DCFH-DA; Sigma-Aldrich) to the fluorescent derivative 2′,7′-dichlorofluorescein (DCF) [23]. Extracellular H2O2 was determined with a microplate assay procedure utilizing the Amplex Red Hydrogen Peroxide/Peroxidase Assay Kit (Invitrogen). Briefly, 100 µL cell supernatant were incubated in a humidified atmosphere and 5% CO2 at 37°C, with HRP (1 U/mL) and Amplex Red for 10 min. Then, the fluorescence was measured using a DTX880 multimode detector microplate reader (Beckman Coulter). The assay was calibrated with authentic H_2O_2 and with quality control samples as described in [24]. Data were mean ± SD of three independent experiments run in six replicates.

2.7. Oil Red O staining

Cellular lipids were measured by Oil Red O (ORO) staining according to [25]. After the treatments the HepaRG cells were fixed in 4% paraformaldehyde (PFA, Leica) for 15 min at room temperature, and then were washed three times with phosphate-buffered saline (PBS, Sigma-Aldrich). Cells were stained with 0.5% ORO

solution (Sigma-Aldrich) for 5 min and then with hematoxylin solution (Sigma-Aldrich) for 1 min. Slides were rinsed with distilled water and then analyzed by optical microscopy. To quantify the cellular content of ORO, the cell pellet was incubated for 10 min with 100 μl of isopropanol and the absorbance of the extract was assessed at 510 nm using a DTX880, Multimode Detector Beckman Coulter reader.

2.8. Lipid droplet assay

Quantitative analysis of cellular lipid droplets (LD) was performed by LipidSpot 610 Lipid Droplet Stain kit (Biotium). The HepaRG cells were fixed with a formaldehyde-based fixative for 10 min at room temperature, and then washed three times with phosphate-buffered saline (PBS, Sigma-Aldrich). Incubation with LipidSpot Lipid Droplet Stain 1X diluted in PBS, was carried out in fixed cells protected from light and maintained at room temperature for 10 min. Imaging analysis was performed using the microplate confocal microscopy system Operetta CLS (Perkin Elmer).

2.9. Gene expression studies

The cellular transcriptome was evaluated using a Human Clariom GO Screen microarray assay and a GeneTitan MC instrument (applied biosystems, Thermo Fisher Scientific). Total RNA was extracted from cells lysates using a QIAsymphony RNA Kit on a QIAsymphony SP instrument (Qiagen). The quality and quantity of RNA were determined with a Nanodrop 2,000 spectrophotometer (Thermo Fisher Scientific) at 260 nm/280 nm absorbance. Integrity of RNA was checked using an RNA 6,000 Pico Kit (Agilent) and all samples had RIN>9.6. Six nanogram of total RNA were used to generate cDNA, then fragmented and labeled cDNA was hybridized to a Human Clariom GoScreen 384-array plate for 17 h at 45°C. Arrays were washed, stained and then scanned using the GeneTitan MC Instrument and CEL Intensity files were generated by Affymetrix GeneChip Command Console Software (AGCC, Thermo Fisher Scientific).

Gene expression analysis was performed using Transcriptomic Analysis Console Software (Thermo Fisher Scientific) that provides quality control analysis, and data normalization and summarization based on the Signal Space Transformation-Robust Multi-Chip Analysis (SST-RMA) algorithm. This provides a list of significant differentially expressed genes (P-value $\leq$ .05); significance was calculated using an Anova with eBayes correction of variance on Limma Bioconductor package (Version 3.15) [26].

Microarray data were used to define the effect of FFA treatment and to compare the effects of VD formulations using the following data-matching strategy (control and experimental groups are as in Fig. 1):

1. [Control test three (FFA treatment) *vs.* Control test one (vehicle DMSO)] to determine the effect of steatosis and lipotoxicity on the cellular transcriptome;
2. [Control test two (VD pretreatment) corrected for Control test three (FFA treatment) *vs.* Control test one (vehicle DMSO)] to discern the protective effect of VD formulations on the FFA-induced lipotoxicity.

2.10. Ingenuity pathway analysis (IPA)

Ingenuity Pathways Analysis (QIAGEN Inc., https://www.qiagenbioinformatics.com/products/ingenuitypathway-analysis) was used to interpret gene expression patterns associated with the response to lipotoxicity and VD formulations. IPA is an aggregator of scientific references that allows searching relevant information on biological and molecular associations between genes/proteins thus identifying their allocation in specific networks of interaction and functional domains.

The "IPA Comparison Core analysis" module was used to interpret the gene expression patterns generated during the cellular treatments considering a gene fold-change cut-off of two (absolute value) [27] and filtering the datasets by selected anatomical and histopathological annotations, namely "liver tissue" and "hepatic cell lines." An IPA activation Z-score > 1.7 or < -1.7 was arbitrarily chosen to capture biological events that significantly match gene patterns described in literature for the selected annotations, and to return significant correlations with biofunction (BF) or cellular effects. Statistical significance (P-value $\leq$ .05) of Z-score data in the different treatments was evaluated using Fisher's Exact Test, right-tailed (P-value $\leq$ .05). The graphical representation of gene networks associated to BFs was obtained using the "IPA Molecule Activity Predictor" tool (MAP).

2.11. Immunoblot

Cells were harvested and suspended in a cell lysis buffer (Cell Signaling Technology) supplemented with protease inhibitor cocktail (Thermo Fisher Scientific) for cellular proteins extraction that was performed by sonication in ice (three cycles of 15 s each with 1 min intervals). After incubation in ice for 1 hr, proteins were recovered by centrifugation of the extracts (12,000 rpm for 20 min at 4°C) and total proteins in the supernatants were quantified using a BCA protein assay kit (Thermo Fisher Scientific). Then, 20 μg of proteins were loaded onto 4–12% SDS–PAGE minigels (Novex WedgeWell Tris-Glycine gel, Invitrogen). After separation, these proteins were blotted and immobilized on a nitrocellulose membrane (Millipore) that was incubated with 5% skim milk (Euroclone) in Tris buffer saline (TBS; 20 mM Tris base, 150 mM NaCl, pH 7.4) and 0.1% Tween-20 for 1 h at room temperature. The blots were incubated with primary antibodies at 4°C overnight under constant shaking and then washed twice with TBS. The primary antibodies were: anti-PXR (1:1,000 dilution, ab192579, abcam), anti-CYP3A4 (1:1,000 dilution; TA324142, OriGene Technologies, Inc., Rockville, MD), anti-FXR (1:500, Santa Cruz Biotechnology, Inc.); anti-CYP24A1 (1:1,000; Boster Bio Rabbit Monoclonal Antibody catalog # M00343); anti-VDR (# 12,550;1:1,000), anti-β-actin (#3,700; 1:1,000), anti-GAPDH (#2,118; 1:2,000) and from Cell Signaling Technology. The secondary antibodies were anti-rabbit (#7,074) or anti-mouse (#7,076) IgG 1:2,000) horseradish peroxidase-linked (Cell Signaling Technology). Protein bands were detected using an ECL Clarity or ECL Clarity Max (BioRad). Quantification of bands was performed with a ChemiDoc Imaging System, Biorad, and protein expression levels were normalized against housekeeping proteins.

2.12. Statistics and graphical representation

Cell biology and biochemistry data were as mean ± S.D. One-way ANOVA was used to assess the variance within groups of cell tests, and paired and unpaired Student's t test was used when appropriate to identify significant differences during the comparison of treatments and phases of treatment (Fig. 1). A probability of error < .05 was considered significant.

Gene data analysis was performed using R software version 4.1.2 (January 11, 2021), platform x86_64-w64-mingw32/x64 (64-bit) running under Windows 10 × 64 (build 19044). Multivariate analysis of normalized gene expression data was performed by independent principal component analysis (IPCA) using the mixOmics package WITH UNSUPERVISED. Results of Differential Expression Analysis (genes differentially expressed in at least one of the comparisons between cell treatments, P-value < .05) were presented as heatmap and Volcano plot charts prepared by Complex Heatmap package and *ggplot2* package, respectively.

3. Results

3.1. Effects of VD formulations on liver cell steatosis and lipotoxicity

The treatment of HepaRG cells with FFA (Fig. 1, control three) was confirmed to induce cellular steatosis and LD formation (Figs. 2A and B). This resulted in increased levels of lipotoxicity as determined by cellular ROS and H_2O_2 efflux (Fig. 2C), and cell viability (Fig. 2D) analysis. Conversely, the pretreatments with the different forms of VD when considered independently form FFA treatment (control test two, Fig. 1) did not significantly affect these parameters (Figs. 2A–D). In the treatment test (Fig. 1), all the three forms of VD significantly reduced the levels steatosis ad lipotoxicity of FFA treated cells (Figs. 2A–D).

3.2. Transcriptomics

Microarray data (available for consultation at https://www-ncbi-nlm-nihgov.ezproxy.upec.fr/geo/browse/?view=series&search=GSE200765&tax=9606&suppl=CEL&display=20) showed that, together, the different forms of VD significantly modulated 2,043 genes in FFA-treated cells; the higher number of entries were observed for SV-VD3 and 1,25$(OH)_2$-D3, with 934 and 721 genes, respectively, whereas SM-VD2 significantly modulated 388 genes (Supplementary Table S1). Volcano plot and heatmap representations of differentially expressed genes (Figs. 3A and B, respectively) demonstrated completely different gene fingerprints in the effect of SM-VD2 and SV-VD3 pretreatments, as well as in the comparison of SV-VD3 and 1,25$(OH)_2$-D3, whereas commonalities were observed between SM-VD2 and 1,25$(OH)_2$-D3 in the top twenty genes identified in the Volcano plot analysis (Supplementary Table S2), which was confirmed by IPCA (Fig. 3C) and Venn diagram representation (Fig. 3D and Supplementary Table S1).

These differences were also highlighted by IPA (Fig. 3E) demonstrating that all the three forms of VD are able to revert the effect of FFA treatment on lipid metabolism (mainly long-chain FA oxidation) and cell viability BFs (upper panel of Fig. 3E and Supplementary Fig. S2), but each VD formulation produced a different

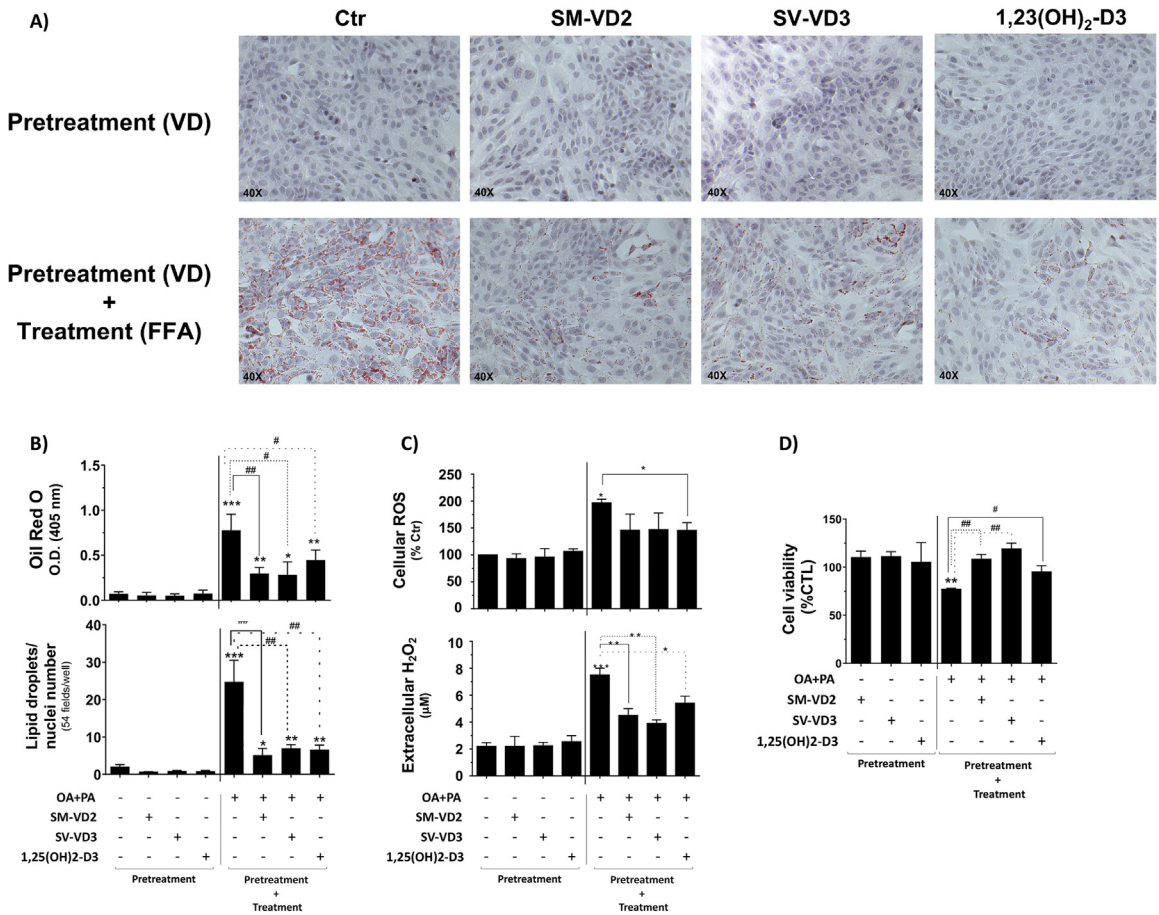

Fig. 2. Effects of vitamin D formulations on the FFA-induced steatosis and lipotoxicity of HepaRG cells. (A) Light microscopy identification of cellular lipids stained with ORO (B); levels of cellular lipids as determined by spectrophotometric analysis of ORO absorbance of cell lysates (upper panel) and lipids droplet quantification by LipidSpot staining and microplate confocal microscopy analysis (lower panel); (C) cellular ROS and extracellular H_2O_2 levels measured by DCFA and Amplex Red fluorescent probes (upper and lower panel, respectively); (D) cell viability assessed by MTT test (E). One-WAY ANOVA or t-test: $^{*}P < .05$, ** $P < .01$ and *** $P < .001$ *vs.* Control 1 test (Ctr); # $P < .05$, ## $P < .01$ and ### $P < .001$ *vs.* FFA treatment. (For interpretation of the references to colour in this figure legend, the reader is referred to the web version of this article.)

gene modulation pattern (shown in detail in Supplementary Table S3) with different number and type of BFs identified in the semantic categories “Metabolism” and “Cell viability” of liver tissue and hepatic cell lines anatomical annotations (Supplementary Fig. S2). More in detail, the differences between SM-VD2 and SV-VD3 consisted in the number of BF modulated for semantic fields (4 BF *vs.* 1 BF in each field, respectively; Supplementary Fig. S2). In the case of SM-VD2, these included the inhibition of BF relevant to long-chain FA oxidation, carbohydrate metabolism and synthesis, hepatocyte damage and cell death (Fig. 3E and Supplementary Fig. S2), whereas SV-VD3 modulated necrosis and phosphatidic acid metabolism BFs (Fig. 3E and Supplementary Fig. S2). Again, SM-VD2, but not SV-VD3, shared with 1,25$(OH)_2$-D3 the modulation of relevant BFs in FFA-treated cells, including the inhibition of long-chain FA oxidation, and carbohydrate metabolism and synthesis BFs (Supplementary Fig. S2). Specific responses of hepatic BFs to 1,25$(OH)_2$-D3 pretreatment in FFA-treated cells were the reduction of lipid and D-glucose biosynthesis, and positive modulation of insulin sensitivity, hypertriglyceridemia and glucose tolerance (lower panel of Fig. 3E and Supplementary Fig. S2).

3.3. Immunoblot of VDR-related genes

Immunoblot was used to verify whether VDR and other VD-related genes can confirm, and eventually explain, the different response of the cellular transcriptome to VD formulations. The list of genes investigated by immunoblot, their functional interaction and the corresponding crude microarray data are shown in Supplementary Fig. S4.

The results showed that the pretreatment with VD formulations, by itself (control test two, Fig. 1), had minor effects on VDR protein expression (Fig. 4A, left side of the blot image and bar chart). However, if VDR protein expression was investigated at a shorter pretreatment time (6 h *vs.* the 24 h of the protocol described in Fig. 1), a significant induction effect on VDR expression was observed for both the natural and synthetic VD formulation (Supplementary Fig. S3, right chart). This finding on VDR protein expression corresponded to increased levels of the *VDR* transcript measured by PCR analysis (Supplementary Fig. S3, left chart), thus suggesting a rapid transcriptional response and protein turnover for this NR in liver cells.

When the FFA treatment was considered independently from VD pretreatments (control test three, Fig. 1), VDR protein expression was markedly induced (Fig. 4A, first line on the right side of the blot image and first bar of the right side of the bar chart). Combining VD pretreatments with FFA treatment (treatment test, Fig. 1), SV-VD3 produced a significant reduction of VDR protein expression, whereas SM-VD2 and 1,25$(OH)_2$-D3 resulted in nonsignificant reductions (Fig. 4A, right side of the bar charts). These findings were coherent with microarray data on VDR expression (Sup-

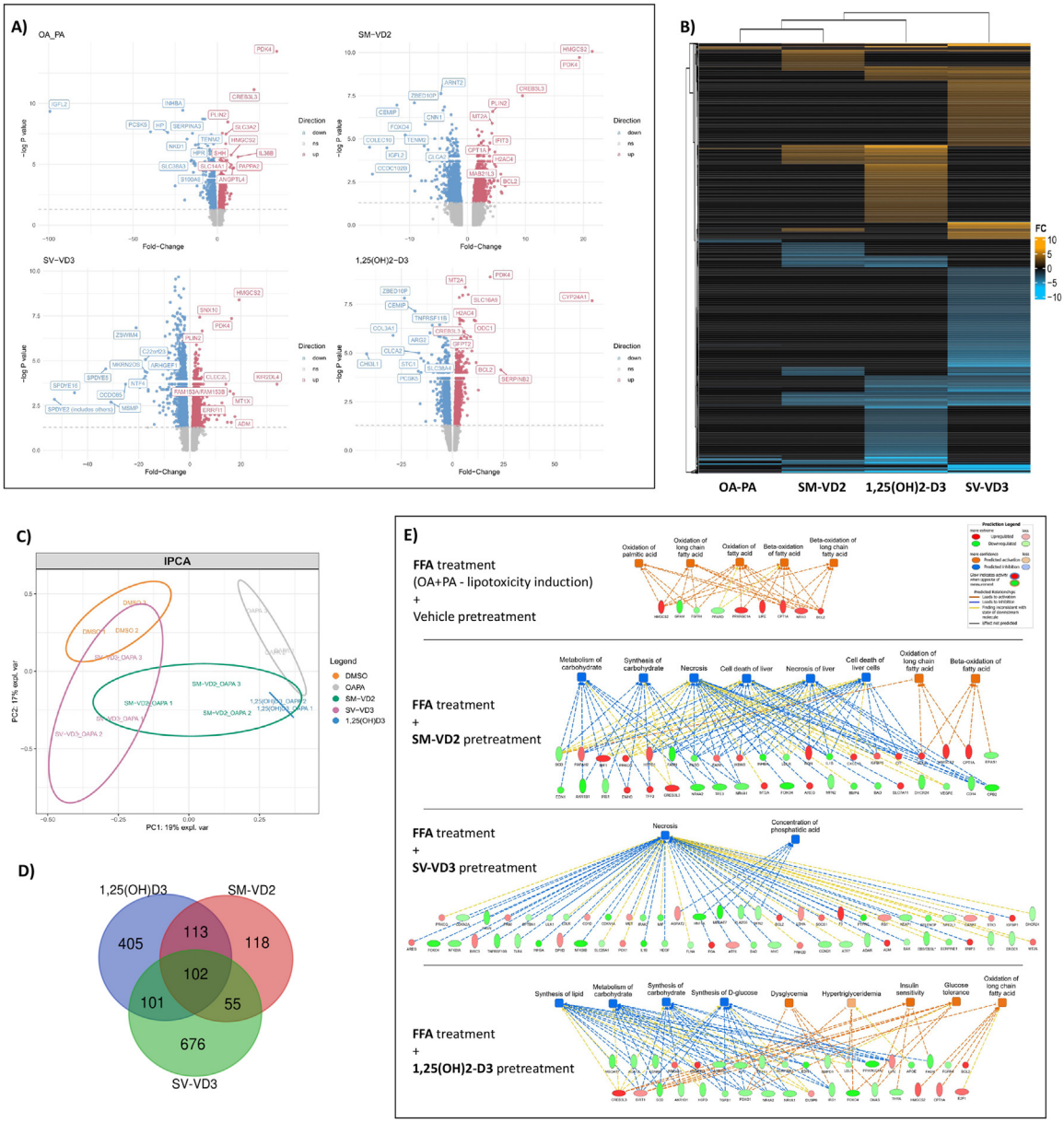

Fig. 3. Analysis of gene microarray data obtained in HepaRG cells pretreated with VD formulations and treated with FFA to induce lipotoxicity. (A) Volcano plot representation of fold change levels of whole genes investigated by microarray technique. Data were corrected for control test 1 (Fig. 1; cells pretreated and treated with the vehicle DMSO) and *Fold-Change* of each gene and its corresponding *minus log10 of the P -value* were represented in the x and y axis, respectively. The top-twenty up and down-regulated genes were identified for each comparison by their score value and were presented by the corresponding gene labels (see also Supplementary Table S2). The horizontal dashed grey line indicates the .05 significance of the *P* -value and the colour of the symbols indicates the significance of the difference with respect to control samples (grey dots represent nonsignificant genes, red dots represent up-regulated genes and blue dots represent down-regulated genes). (B) Heatmap chart of differentially expressed genes in the four groups of data compared in this study. Colours identify the Fold-Change (FC) levels and their significance with respect to control test 1 (Fig. 1); black represents nonsignificant genes, orange represents up-regulated genes and blue represents down-regulated genes. (C) IPCA of matrices of differentially expressed genes in the four experimental groups considered in the study. The datasets corresponding to the different groups were identified by the colour of labels, and their clusterization and spatial distribution was described by ellipsoids that represent the 95% confidence level. (D) Venn Diagram of differentially expressed genes in the pretreatments with the three different forms of VD. Gene datasets were: natural VD2 formulation (SV-VD2), synthetic VD3 formulation (SM-VD3) and VD3 bioactive metabolite 1,25(OH)$_2$-D3; the corresponding list of genes are reported in Supplementary Table S1. Gene expression data were corrected for the control test three (Fig. 1; cells pretreated with DMSO and then treated with FFA). (E) Ingenuity Pathway Analysis (IPA) was carried out by comparison core analysis on significantly modulated genes (fold change cut-off = 2) filtered by "liver tissue" and "hepatic cell lines" annotations. The transcriptional response to the VD pretreatments and FFA treatment was corrected for the response observed in control test 1 (Fig. 1; cells treated with the vehicle DMSO). Gene modulations and clusterization into specific biological functions identified by IPA are shown in Supplementary Table S3. (For interpretation of the references to colour in this figure legend, the reader is referred to the web version of this article.)

plementary Fig. S4 A), suggesting that the modulation of VDR, by itself, is not sufficient to explain the effect of VD formulations on the FFA-induced lipotoxicity of HepaRG cells.

Indeed, the lipotoxicity process is expected to affect VDR expression and activity by influencing the complex series of molecular and functional interactions of this NR with other cellular proteins. These include other nuclear receptors and transcriptional proteins important in the hepatic metabolism and detoxification of cellular lipids, including VD analogues and metabolites, as well as in bile acid signaling, and in the regulation of energy metabolism

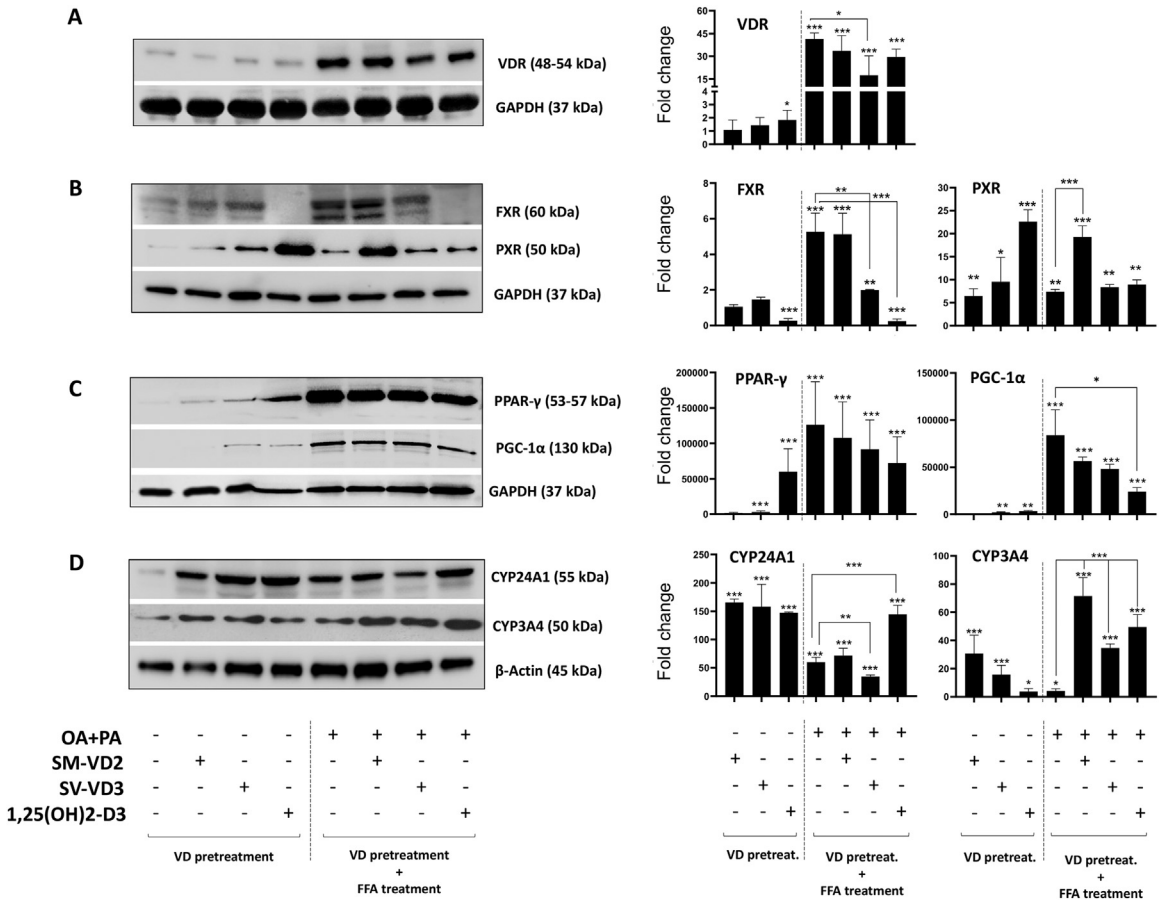

Fig. 4. Immunoblot of VDR and other vitamin D-related proteins. The proteins investigated by immunoblot were: (A) VDR; (B) FXR and PXR; (C) PPARγ and PGC-1α transcriptional coactivator; (D) CYP24A1 and CYP3A4. Corresponding microarray data and functional interactions are shown in Supplementary Fig. S4A and S4B. One-WAY ANOVA or t-test: * $P < .05$, ** $P < .01$ and *** $P < .001$. Statistical comparisons were: (symbols on top of error bars) *vs.* Control 1 test (Fig. 1, vehicle DMSO); (symbols on top of horizontal connectors) *vs.* Control test three (Fig. 1, FFA treatment presented in the first bar of the right side of the charts).

and inflammatory pathways (Fig. 4 and Supplementary Fig. S4) [28,29]. Assessing the expression of some of these VDR-interacting proteins, namely FXR, PXR, PPARγ and PGC-1α, and that of their reporter genes involved in VD metabolism, namely the CYP450 isoenzymes 24A1 and 3A4 (Fig. 4), the response to SM-VD2 and SV-VD3 pretreatments in FFA-treated hepatocytes was markedly different and apparently unrelated to a single-gene or target-specific effect.

More in detail, when the VD pretreatments were studied independently from FFA treatment (control 2, Fig. 1), 1,25(OH)$_2$-D3 was observed to inhibit FXR expression (Fig. 4B, left side of immunoblot images and bar charts), whereas the expression of all the other proteins was induced with the pecking order 1,25(OH)$_2$-D3 > SV-VD3 > SM-VD2 (Figs. 4B and C); all the VD formulations enhanced the expression of CYP24A1 whereas CYP3A4 levels increased with the order SM-VD2 > SV-VD3 > 1,25(OH)$_2$-D3 (Fig. 4D).

Likewise to VDR protein, the receptor proteins FXR and PPARγ, and the transcriptional coactivator PGC-1α were significantly up-regulated in FFA-treated cells (treatment test, Fig. 1); these findings are shown in Figs. 4B and C (first line of the blots and first bar of the charts on the right side). 1,25(OH)$_2$-D3 almost completely ablated this effect of FFA on FXR protein expression (right side of Fig. 4B) also reducing PGC-1α expression (right side of Fig. 4C); SV-VD3 pretreatment significantly decreased FXR expression, whereas SM-VD2 markedly induced PXR expression (Fig. 4B). All the VD pretreatments, and especially SM-VD2, induced CYP3A4 expression of FFA-treated cells (Fig. 4C, right bar chart) whereas 1,25(OH)$_2$-D3 enhanced, and SV-D3 reduced, CYP24A1 protein expression (Fig. 4D, left).

4. Discussion

Vitamin D shows antiproliferative, anti-inflammatory and antifibrotic properties that have demonstrated to help preventing NAFLD in a plethora of *in vitro* and *in vivo* studies (recently reviewed in [11]). A growing body of evidence suggests a causal relationship between vitamin D deficiency and NAFLD, with low levels of 25(OH)D that are associated with hepatic inflammation, severity of NAFLD and its progression to NASH [15,16]. At the same time, VD deficiency could be a consequence of NAFLD and NASH, since liver dysfunction may directly interfere with the hepatic metabolism of VD to form 25(OH)-D3 or 25(OH)-D2 [30]. These pieces of evidence support the notion that VD supplementation may help to prevent NAFLD and its progression to NASH. In fact, VD has been listed among the nutraceuticals that, if well dosed and administered for a sufficient time and in association to lifestyle changes, could have beneficial effects on NAFLD and NAFLD-related parameters [15]. Several VD formulations are available for this purpose that appear to be safe over a wide range of dosages up to megadoses [9]. However, no specific indication on the form of VD to use is present in literature, and these include natural VD formulations [2] developed by food and pharmaceutical companies to respond to the increased demand of natural nutrients and supplements [31]. However, the efficacy of specific formulations to pre-

vent or cure NAFLD and NASH, remains poorly characterized. This lack of knowledge is compounded by the paucity of studies on the effect that VD may have on liver cell lipotoxicity, the actual pathogenic instigator of NAFLD [14]. Therefore, these aspects are worth investigating at the preclinical level.

In this study we compared natural (VD2-containing Shitake extract) and synthetic (pure VD3) formulations of VD in protecting human liver cells against FFA-induced lipotoxicity [25,32]. We found that both the two formulations and their bioactive analogue 1,25(OH)$_2$-D3, prevent FFA-induced lipotoxicity of human liver cells reducing at the same time lipid synthesis and sequestration (lipid droplets levels), and the ROS generating response of these cells (Fig. 2).

Gene microarray data unequivocally demonstrated that the cytoprotective properties of the different VD formulations were associated with the modulation of different groups of genes all important to restore the metabolic homeostasis and to confer increased resistance to the cytopathic effects of lipotoxicity by necrotic and apoptotic cell death. These findings are in agreement with transcriptomics data obtained in a recent study performed in human microvascular endothelial cells in which a low-dose VD treatment was identified to prevent palmitate lipotoxicity modulating groups of genes involved in the same cytoprotective processes, including the cellular stress response, cell cycle regulation, and DNA replication and repair [33].

Important was the finding that gene microarray fingerprints of 1,25(OH)$_2$-D3 and SM-VD2 and their biological interpretation by IPA, showed some similarities, suggesting VD-like activity for this natural formulation. Conversely, the response to SV-VD3 in FFA-treated cells was completely different from that of 1,25(OH)$_2$-D3. These differences were observed in the identity of significantly modulated genes (Figs. 3A–C and Supplementary Table S2), as well as in their number (934 in SV-VD3 *vs.* 388 of SM-VD2 and 721 of 1,25(OH)$_2$-D3 pretreatment; Fig. 3D and Supplementary Table S1), and in the number and identity of affected BFs retrieved by IPA among liver tissue and hepatic cell annotations. In the case of SV-VD3 these were restricted to cellular necrosis and phosphatidic acid metabolism, whereas in the case of SM-VD2 these included necrotic cell death, long-chain fatty acid oxidation, and carbohydrate metabolism and synthesis. Essentially, the gene homology between SM-VD2 and 1,25(OH)$_2$-D3 pretreatment regarded metabolic BFs (Fig. 3E and Supplementary Table S2). Also, 1,25(OH)$_2$-D3 was found to affect other hepato-metabolic BFs with key role in NAFLD [34], as insulin sensitivity, glucose tolerance, dysglycemia and hypertriglyceridemia.

These differences between SM-VD2 and SV-VD3 are difficult to explain on the bases of the form of VD present in these formulations, namely ergocalciferol and cholecalciferol, and their VD activity. In fact, the actual bioactive metabolite of D2 and D3, namely 1,25(OH)$_2$-D, cannot form to significant levels in liver cells (Supplementary Fig. 1A); these mainly express 25-hydroxylase enzymatic activity by CYP2R1 [30] and other CYP450 isoforms, such as CYP3A4 that has been identified as a human microsomial vitamin D 25-hydroxylase [35]. However, even if the bioactive metabolites of D2 and D3 are formed to some extent in liver cells, these have similar VDR binding affinity and molecular responses [36], which is opposite to the type of response observed for SM-VD2 and SV-VD3 in the present study. Therefore, under the experimental conditions of this study, it is unlikely that SMVD2 and SV-VD3 may act on the liver cell transcriptome by means of the transformation of their vitamers to the corresponding 1,25(OH)$_2$ metabolites; the comparison of gene array data of 1,25(OH)$_2$-D3 with those of SM-VD2 and SV-VD3 pretreatments, confirms this assumption.

To shed further light on these aspects, we measured the expression of VDR and other proteins that interact with this NR in order to control the molecular and metabolic response to VD. These include nuclear receptors that transactivate via RXR/RAR heterodimerization, such as FXR, PXR and PPARγ, the PPARγ transcriptional coactivator PGC-1α and two reporter genes of these receptors with proven role in VD metabolism, namely CYP24A1 and CYP3A4. VDR and FXR are both activated by bile acids and their interaction plays important roles in the control of the gut-liver axis, hepatic inflammation and insulin function [29]; PXR is a member of the VDR-like group of NR, important in the transcriptional regulation of lipid metabolism and detoxification genes of the liver cell as well as of other cell types including intestinal and neuronal cells [37,38]. The transactivation of these NR controls CYP450 isoenzymes important in the catabolism of VD, as CYP24A1 [39], and in the pleiotropic response of the human liver to a broad spectrum of lipophilic xenobiotics and lipid metabolites, including 1,25(OH)2-D3 [28]. In this respect, this network of NR is known to control the expression of CYP3A4 and other CYP3A isoenzymes with vitamin D 25 hydroxylase activity [28,35,40]. Also, VDR, its homologues of the NR1I family, such as PXR, and FXR interact to control the response to nutrients in the liver cell, regulating the insulin signaling and the transcriptional activity of PGC-1α on *PPAR*γ. The latter is a key homeostatic player of the liver and adipose tissue, regulating the flux of long-chain FA towards energy accumulation by the biosynthesis and sequestration of triglycerides, or energy production by lipid oxidation processes [25,32,41]; also, PPARγ is a pharmacological target for hepatic lipotoxicity, inflammation and liver cell death associated with NAFLD [42].

Immunoblot data on this array of VDR-related proteins confirmed the different response to SM-VD2 and SV-VD3 formulations in FFA-treated cells. SM-VD2 was characterized by a marked induction of PXR and CYP3A4 expression (Figs. 4B and D), pointing to an increased detoxification potential and 25-hydroxylase activity of liver cells. Conversely, SV-VD3 significantly reduced VDR (Fig. 4A) and FXR expression (Fig. 4B) that was markedly upregulated by FFA treatment to sustain lipogenesis and lipotoxicity mechanisms [43]. SV-VD3 also reduced the expression of the VD catabolism protein CYP24A1 (Fig. 4D), which may have therapeutic relevance in VD deficiency states [44]. Commonalities between 1,25(OH)$_2$-D3 and SV-VD3 were the inhibition of FXR expression, and between 1,25(OH)$_2$-D3 and SM-VD2 the absence of a significant inhibition of VDR. At the same time, all the three forms of VD activated the expression of CYP3A4, which may represent a converging detoxification response for these forms to prevent FFA-induced lipotoxicity.

Furthermore, the fact that only 1,25(OH)$_2$-D3 activated protein expression and reduced gene transcription of CYP24A1 (Fig. 4D and Supplementary Table S2), confirms that the expression of this CYP450 isoforms marks VD activity in human liver cells. Other characteristic responses to 1,25(OH)$_2$-D3 pretreatment included the complete inhibition of FXR and the significant reduction of PGC1a protein expression (Figs. 4B and C), which may explain the convergence of all gene modulation effects of this VD metabolite on metabolic BFs of FFA-treated cells (Fig. 3E and Supplementary Fig. S2). Again, these findings highlight that metabolic BFs in common between 1,25(OH)$_2$-D3 and SM-VD2, and identified by IPA as relevant to liver cell protection, can be activated through different and apparently VDR-independent pathways that include FXR/PGC-1a inhibition and PXR activation, respectively.

Altogether these findings demonstrate that natural and synthetic formulations of VD prevent lipotoxicity of human liver cells activating different networks of genes and VDR-related proteins. Gene fingerprints suggest that the natural formulation SM-VD2 and the bioactive metabolite 1,25(OH)$_2$-D3 have in common the expression of a significant number of genes useful in preventing hepatic lipotoxicity; such commonalities highlight VD-like properties

for SM-VD2 that are apparently independent from VDR activity and absent in the synthetic formulation containing pure VD3. It is conceivable to imagine that these differences can be the consequence of the biological complexity of the natural extract [45] that in addition to ergocalciferol include other components of Shitake raw material. These components are worth investigating further at the preclinical and clinical level as far as their functional complexity and biological impact on lipotoxicity are regarded.

Author statement

Here we declare that the authors Tiziana Frammartino, Angela Guerrini, Stefano Garetto, Jacopo Lucci and Isabelle Franco Moscardini are employees of Bios-Therapy, Physiological Systems For Health S.p.A., Loc. Aboca 20, 52037 Sansepolcro, AR, Italy.

Author contributions

FG, DB, SG and JL conceived and designed the experiments;
DB, TF, AMS, AM, AG, LZ, GM performed the experiments;
DB, SG, IFM and JL analyzed and interpreted the data;
MR, JL and FG contributed reagents, materials, analysis tools or data;
DB, SG, JL and FG wrote the paper.

Declaration of competing interests

Tiziana Frammartino, Angela Guerrini, Stefano Garetto, Jacopo Lucci and Isabelle Franco Moscardini are employees of Bios-Therapy, Physiological Systems For Health S.p.A., Loc. Aboca 20, 52037 Sansepolcro, AR, Italy. The rest of the authors declare that they have no conflicts of interest.

Supplementary materials

Supplementary material associated with this article can be found, in the online version, at doi:10.1016/j.jnutbio.2023.109319.

References

[1] Hernigou P, Sitbon J, Dubory A, Auregan JC. Vitamin D history part III: the "modern times"-new questions for orthopaedic practice: deficiency, cell therapy, osteomalacia, fractures, supplementation, infections. Int Orthop 2019;43(7):1755–71.
[2] Urena-Torres P, Souberbielle JC. Pharmacologic role of vitamin D natural products. Curr Vasc Pharmacol 2014;12(2):278–85.
[3] Gil A, Plaza-Diaz J, Mesa MD. Vitamin D: classic and novel actions. Ann Nutr Metab 2018;72(2):87–95.
[4] Bouillon R, Marcocci C, Carmeliet G, Bikle D, White JH, Dawson-Hughes B, et al. Skeletal and extraskeletal actions of vitamin D: current evidence and outstanding questions. Endocr Rev 2019;40(4):1109–51.
[5] Maretzke F, Bechthold A, Egert S, Ernst JB, Melo van Lent D, Pilz S, et al. Role of vitamin D in preventing and treating selected extraskeletal diseases-an umbrella review. Nutrients 2020;12(4):969.
[6] Bleizgys A., Vitamin D dosing: basic principles and a brief algorithm (2021 update), Nutrients, 2021, 13(12)4415.
[7] Kimball SM, Holick MF. Official recommendations for vitamin D through the life stages in developed countries. Eur J Clin Nutr 2020;74(11):1514–18.
[8] Sempos CT, Heijboer AC, Bikle DD, Bollerslev J, Bouillon R, Brannon PM, et al. Vitamin D assays and the definition of hypovitaminosis D: results from the first international conference on controversies in vitamin D. Br J Clin Pharmacol 2018;84(10):2194–207.
[9] Narvaez J, Maldonado G, Guerrero R, Messina OD, Rios C. Vitamin D megadose: definition, efficacy in bone metabolism, risk of falls and fractures. Open Access Rheumatol 2020;12:105–15.
[10] Guessous I. Role of vitamin D deficiency in extraskeletal complications: predictor of health outcome or marker of health status? Biomed Res Int 2015;2015:563403.
[11] Pacifico L, Osborn JF, Bonci E, Pierimarchi P, Chiesa C. Association between vitamin D levels and nonalcoholic fatty liver disease: potential confounding variables. Mini Rev Med Chem 2019;19(4):310–32.
[12] Younossi ZM, Golabi P, de Avila L, Paik JM, Srishord M, Fukui N, et al. The global epidemiology of NAFLD and NASH in patients with type 2 diabetes: a systematic review and meta-analysis. J Hepatol 2019;71(4):793–801.
[13] Jayakumar S, Loomba R. Review article: emerging role of the gut microbiome in the progression of nonalcoholic fatty liver disease and potential therapeutic implications. Aliment Pharmacol Ther 2019;50(2):144–58.
[14] Svegliati-Baroni G, Pierantonelli I, Torquato P, Marinelli R, Ferreri C, Chatgilialoglu C, et al. Lipidomic biomarkers and mechanisms of lipotoxicity in non-alcoholic fatty liver disease. Free Radic Biol Med 2019;144:293–309.
[15] Cicero AFG, Colletti A, Bellentani S. Nutraceutical approach to non-alcoholic fatty liver disease (NAFLD): the available clinical evidence. Nutrients 2018;10(9):1153.
[16] Wang X, Li W, Zhang Y, Yang Y, Qin G. Association between vitamin D and non-alcoholic fatty liver disease/non-alcoholic steatohepatitis: results from a meta-analysis. Int J Clin Exp Med 2015;8(10):17221–34.
[17] Torquato P, Bartolini D, Giusepponi D, Piroddi M, Sebastiani B, Saluti G, et al. Increased plasma levels of the lipoperoxyl radical-derived vitamin E metabolite α-tocopheryl quinone are an early indicator of lipotoxicity in fatty liver subjects. Free Radic Biol Med 2019;131:115–25.
[18] Schmolz L, Schubert M, Kirschner J, Kluge S, Galli F, Birringer M, et al. Long-chain metabolites of vitamin E: Interference with lipotoxicity via lipid droplet associated protein PLIN2. Biochim Biophys Acta 2018;1863(8):919–27.
[19] Bartolini D, Torquato P, Barola C, Russo A, Rychlicki C, Giusepponi D, et al. Nonalcoholic fatty liver disease impairs the cytochrome P-450-dependent metabolism of α-tocopherol (vitamin E). J Nutr Biochem 2017;47:120–131.
[20] Bartolini D., R. Marinelli, A. Stabile, T. Frammartino, A. Guerrini, S. Garetto, et al. (2022). The nutrigenomics signature of wheat germ oil vitamin E in oleic acid- induced lipotoxicity of huma liver cells. Free Radic Biol Med.
[21] Bartolini D, Piroddi M, Tidei C, Giovagnoli S, Pietrella D, Manevich Y, et al. Reaction kinetics and targeting to cellular glutathione S-transferase of the glutathione peroxidase mimetic PhSeZnCl and its D,L-polylactide microparticle formulation. Free Radic Biol Med 2015;78:56–65.
[22] Bartolini D, Commodi J, Piroddi M, Incipini L, Sancineto L, Santi C, et al. Glutathione S-transferase pi expression regulates the Nrf2-dependent response to hormetic diselenides. Free Radic Biol Med 2015;88(Pt B):466–80.
[23] Volpi C, Bartolini D, Brighenti V, Galli F, Tiecco M, Pellati F, et al. Antioxidant power on dermal cells by textiles dyed with an onion (allium cepa l.) skin extract. Antioxidants (Basel) 2021;10(11):1655.
[24] Bartolini D, Arato I, Mancuso F, Giustarini D, Bellucci C, Vacca C, et al. Melatonin modulates Nrf2 activity to protect porcine pre-pubertal Sertoli cells from the abnormal H. J Pineal Res 2022;73(1):e12806.
[25] Bartolini D, Torquato P, Barola C, Russo A, Rychlicki C, Giusepponi D, et al. Nonalcoholic fatty liver disease impairs the cytochrome P-450-dependent metabolism of alpha-tocopherol (vitamin E). J Nutr Biochem 2017;47:120–31.
[26] Ritchie ME, Phipson B, Wu D, Hu Y, Law CW, Shi W, et al. limma powers differential expression analyses for RNA-sequencing and microarray studies. Nucleic Acids Res 2015;43(7):e47.
[27] Krämer A, Green J, Pollard J, Tugendreich S. Causal analysis approaches in ingenuity pathway analysis. Bioinformatics 2014;30(4):523–30.
[28] Noh K, Chow ECY, Quach HP, Groothuis GMM, Tirona RG, Pang KS. Significance of the vitamin D receptor on crosstalk with nuclear receptors and regulation of enzymes and transporters. AAPS J 2022;24(4):71.
[29] Thibaut MM, Bindels LB. Crosstalk between bile acid-activated receptors and microbiome in entero-hepatic inflammation. Trends Mol Med 2022;28(3):223–36.
[30] Cheng JB, Levine MA, Bell NH, Mangelsdorf DJ, Russell DW. Genetic evidence that the human CYP2R1 enzyme is a key vitamin D 25-hydroxylase. Proc Natl Acad Sci U S A 2004;101(20):7711–15.
[31] Ahuja K. VITAMIN E MARKET SIZE BY PRODUCT (SYNTHETIC VITAMIN E, NATURAL VITAMIN E [TOCOPHEROL, TOCOTRIENOLS])... Vitamin E Market Size By Product (Synthetic Vitamin E, Natural Vitamin E [Tocopherol, Tocotrienols]), By Application (Animal Nutrition, Human Nutrition/Dietary Supplements, Functional Food & Beverages, Cosmetics), Industry Analysis Report, Regional Outlook, Growth Potential. Price Trend, Competitive Market Share & Forecast 2020;2020:2026..
[32] Schmölz L, Schubert M, Kirschner J, Kluge S, Galli F, Birringer M, et al. Long-chain metabolites of vitamin E: interference with lipotoxicity via lipid droplet associated protein PLIN2. Biochim Biophys Acta Mol Cell Biol Lipids 2018;1863(8):919–27.
[33] Peters KM, Borradaile NM. Microarray data and pathway analyses for human microvascular endothelial cells supplemented with low dose vitamin D or niacin during lipotoxicity. Data Brief 2019;26:104490.
[34] Barchetta I, Cimini FA, Cavallo MG. Vitamin D and metabolic dysfunction-associated fatty liver disease (MAFLD): an update. Nutrients 2020;12(11).
[35] Gupta RP, Hollis BW, Patel SB, Patrick KS, Bell NH. CYP3A4 is a human microsomal vitamin D 25-hydroxylase. J Bone Miner Res 2004;19(4):680–8.
[36] Bikle DD. Vitamin D metabolism, mechanism of action, and clinical applications. Chem Biol 2014;21(3):319–29.
[37] Bartolini, D., F. De Franco, P. Torquato, R. Marinelli and B. Cerra (2020). "Garcinoic acid is a natural and selective agonist of pregnane X receptor." 63(7): 3701-3712.
[38] Marinelli R, Torquato P, Bartolini D, Mas-Bargues C, Bellezza G, Gioiello A, et al. Garcinoic acid prevents beta-amyloid (Abeta) deposition in the mouse brain. J Biol Chem 2020;295(33):11866–76.

[39] Zhou C, Assem M, Tay JC, Watkins PB, Blumberg B, Schuetz EG, et al. Steroid and xenobiotic receptor and vitamin D receptor crosstalk mediates CYP24 expression and drug-induced osteomalacia. J Clin Invest 2006;116(6):1703–12.
[40] Khan AA, Chow EC, van Loenen-Weemaes AM, Porte RJ, Pang KS, Groothuis GM. Comparison of effects of VDR versus PXR, FXR and GR ligands on the regulation of CYP3A isozymes in rat and human intestine and liver. Eur J Pharm Sci 2009;37(2):115–25.
[41] Nakamura MT, Yudell BE, Loor JJ. Regulation of energy metabolism by long-chain fatty acids. Prog Lipid Res 2014;53:124–44.
[42] Puengel T, Liu H, Guillot A, Heymann F, Tacke F, Peiseler M. Nuclear receptors linking metabolism, inflammation, and fibrosis in nonalcoholic fatty liver disease. Int J Mol Sci 2022;23(5):2668.
[43] Caron S, Huaman Samanez C, Dehondt H, Ploton M, Briand O, Lien F, et al. Farnesoid X receptor inhibits the transcriptional activity of carbohydrate response element binding protein in human hepatocytes. Mol Cell Biol 2013;33(11):2202–11.
[44] Alshabrawy AK, Cui Y, Sylvester C, Yang D, Petito ES, Barratt KR, et al. Therapeutic potential of a novel vitamin D. Biomolecules 2022;12(7):960.
[45] Parisio C, Lucarini E, Micheli L, Toti A, Di Cesare Mannelli L, Antonini G, et al. Researching New Therapeutic Approaches for Abdominal Visceral Pain Treatment: Preclinical Effects of an Assembled System of Molecules of Vegetal Origin. Nutrients 2019;12(1):22.